Chapter 12
Gas-Solid Catalytic Reactions

This chapter will focus in more details on reactions between components in the gas phase catalyzed by a solid catalyst. The chapter will use the basic concepts learned in earlier chapters and show the technological and design application to gas-solid reactions.

The outline of this chapter is as follows: *.1 will show some application areas together with the number of types of reactors available for carrying out gas-solid catalyzed reactions. Section *.2 will focus on the kinetic models suitable for describing these reactions. Section *.3 will show how to set up the reactor models and will also show the mass transport interactions need to be modeled. These transfer effects are then shown in detail in Section *.4 and then applied to design in Section *.5.

The education objectives of this chapter are as follows:

- To gain an overview of various technologies where catalytic reactors are used.
- To assess the relative merits of various types of reactors.
- To model transport effects in packed beds and monolith reactors.
- To perform a preliminary design or sizing of these reactors.

Application Areas

Automobile Emission Control

Catalytic converters used in controlling the exhaust emission is an example of a gas-solid catalytic reaction. The exhaust gases contain high concentrations of hydrocarbons and carbon monoxide. These are reduced by contacting these gases over a solid catalyst; usually an alumina supported Pt catalyst. The catalyst may be placed in a packed bed arrangement or as a monolithic. The schematic of the packed bed arrangements is shown in Figure 1. Here the solid catalyst is held between two retaining grids of inert material. The catalyst beads (usually 3mm diameter with surface area of 100 m^2/g) are housed in a container with large front area and shallow depth. The pressure drop across the catalyst has to be kept to a minimum to ensure an easy flow of the exhaust gases through the converter. Unlike packed beds the monoliths operate at low velocity (laminar flow) and have low pressure drop.

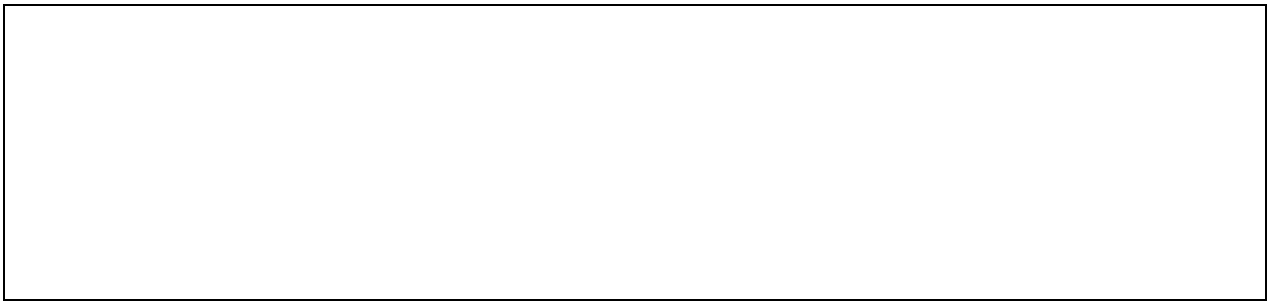

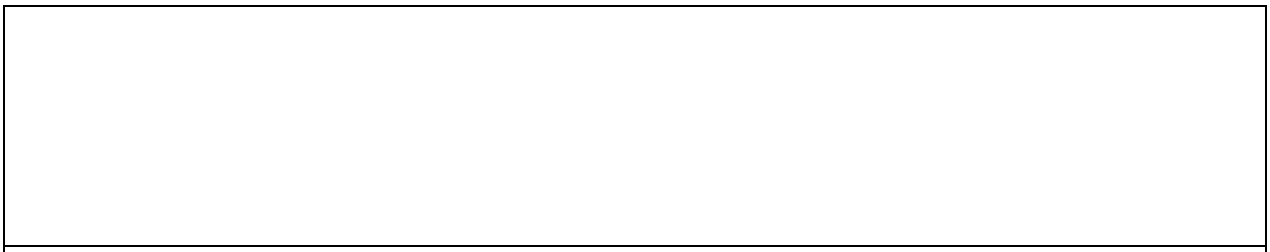

FIGURE 1: Cutaway view of GM packed-bed converter.

The monolith arrangement shown in Figure 2 consists of thin walled parallel channels. These channels are made of high temperature resistant ceramic (cordierite $2MgO.2Al_2O_3.5SiO_2$) or a stainless steel (Fe-Cr-Al-y alloy) and coated with an active catalyst such as Pt.

Catalytic Oxidation of VOCs

VOCs (Volatile Organic Compounds) are a common source of pollutants present in many industrial process stack gas streams and include a variety of compounds depending on the process industry. The catalytic oxidation removes these pollutants at a lower temperature compared to thermal incineration. The operating temperatures are between 600 °F to 1200 °F. Catalyst is a precious metal dispersed with a high surface area work coats. These are then bonded to ceramic honeycomb blocks so that the pressure drop through the catalytic reactor can be kept low. Special proprietary formulations are needed to treat halogenated and sulfur compounds. A typical flow diagram is shown in Figure 3 and the system includes a heat recovery arrangement. Costs for catalytic oxidation depend on many different factors: (i) VOC to be controlled (ii) required destruction efficiencies (iii) operating mode and supplemental fuel needed, etc. Because VOC oxidation occur at lower temperatures, the capital costs are lower than that for thermal oxidation.

FIGURE 2: Monolith catalytic converters for automobile applications.

FIGURE 3: Catalytic oxidation of VOCs.

Selective Catalytic Reduction

SCR (Selective Catalytic Reduction) refer to reduction of a nitrous oxide to nitrogen by reacting with ammonia in presence of a solid catalyst. Boiler exhaust gases contain NO_x as a pollutant and SCR can be used, for example, to treat such streams. The reaction can be represented as:

$$NO_x + 2\frac{x}{3} NH_3 \rightarrow x\, H_2O + \left(\frac{x}{3} + 1\right) N_2$$

An illustrative flowsheet for the process is shown in Figure 4.

The SCR system consists of an ammonia injection grid, catalyst reactor and associated auxiliary equipment. The catalyst is composed of oxides of vanadium, titanium or molybdenum or zeolite based formulations. The catalyst is supplied as a ceramic or metallic honeycomb structure to minimize flue gas pressure drop. Both anhydrous and aqueous ammonia have been used in actual applications. The flue gases must have at least 1% oxygen for the process to operate efficiently.

An important design consideration in these types of reactors is the ammonia slip. Theoretically the amount of ammonia to be injected should be based on a molar ratio of ammonia to NO_x (which is related to the NO_x removal efficiency.) However, since NH_3 is not completely and uniformly mixed with NO_x more than the theoretical quantity is normally injected. The excess residual ammonia in the downstream flue gas is known as ammonia slip.

The NO_x removal efficiency increases with increasing NH_3 slip and reaches an asymptotic value at a certain level of excess NH_3. However, large NH_3 slip is environmentally harmful as indicated below.

(i) Excess NH_3 is environmentally harmful when discharged to the atmosphere through the stack

(ii) Sulfur containing fuels produce SO_2 and SO_3. Small quantity of SO_2 is converted to SO_3 in SCR. In the presence of water vapor and excess NH_3, ammonium sulphate is formed.

$$SO_3 + 2NH_3 + H_2O \rightarrow (NH_4)_2 SO_4$$
$$SO_3 + NH_3 + H_2O \rightarrow (NH_4)HSO_4$$

Ammonium sulfate is powdery and contributes to the quantity of particulates in the flue gas. Also ammonium bisulfate is a sticky substance which deposits on catalyst wall and blocks the flow. (and downstream equipment). The reaction engineering guidelines are useful to optimize the NH_3 slip.

Other problems of importance in the design are variations temperature and flow rate, NO_x and ammonia loading. Process streams may contain particulates, even after dust removal and this could cause clogging especially in a monolith type reactor. Another problem is precipitation of ammonium nitrate which needs to be avoided. Thermodynamics equilibrium calculations are useful to predict conditions of ammonium nitrate formation.

Reactor Types

In the previous section, we mentioned a number of reactors used for gas-solid reactions. We provide some additional details and some design issues for each type of reactor.

1. Packed Beds

These are cylindrical tubes packed with beads of catalyst. The catalyst is usually a porous material with large surface area. Most of the area is inside and hence the reactants have to diffuse into the catalyst for reaction to take place. This can often limit the rate of reaction and is referred to as pore diffusional resistance. The pore resistance leads to a poorer catalyst utilization as the interior of the catalyst is exposed to a much lower reactant concentration than the surface. Detailed analysis of this is provided in a later section. The pore diffusion resistance can be minimized by using smaller diameter particles but one then pays a penalty in terms of increased pressure drop in the bed leading to an increased operational cost. The pressure drop is often a limiting factor in many applications especially for catalytic oxidation of VOC where the gases to be treated are often available at near atmospheric pressures. Thus the optimum design of packed bed is often a compromise between lower pressure drop (lower operating cost) vs. increased utilization of the catalyst (lower capital costs).

If the VOC concentrations are sufficiently high, the recovery of the heat released in the reaction may be important and lead to some energy savings. Some complex modes operations of the packed beds such as regenerative mode have been suggested in the literature to achieve the heat integration needs. Such reactors operate in a periodic mode with the inlet flow switched to either side of the reactor on a periodic basis.

2. Monolith Reactor

Monoliths are thin walled parallel channels with the wall surfaces coated with a catalyst. Such systems are known as wash-coated monoliths. The surface area per unit volume is low in such systems compared to a packed bed and hence these are suitable for reactions which are fast and do not require a high catalyst loading. The pressure drop is lower than packed beds which is an added advantage. The fabrication costs are higher for monolith compared to packed beds.

For systems requiring a high surface area, the porous walled monoliths are useful. Here a thick walled porous matrix is impregnated with active metals such as Pt or Pd and the entire matrix is catalytically active. Again the pressure drop is low but compared to wall coated monolith this system will have some internal pore diffusional resistance.

3. Fluidized Beds

In this mode of operation a high velocity gas stream contacts with fine particles of catalyst and the catalyst bed is in a state of motion and is said to be fluidized. The pressure drop is constant and is independent of the operating gas velocity. Thus the fluidized bed is able to handle a wide range of fluctuations in flow rate. The entire reactor is well mixed leading to efficient contacting of the catalyst with solid fines. Since fine sized catalyst are used, internal resistances are considerably reduced leading to a better utilization of the catalyst. Thus fluidized bed reactors have a number of advantages. The disadvantages are mainly the catalyst attrition leading to dust formation and catalyst carry over. Some gas phase bypassing is also possible leading to a lower conversion compared to packed beds or monoliths.

Some advantages of the fluidized bed reactor are as follows:

1. Uniform temperature in the reactor. Hence if there is a range of optimum operating temperature, then the reactor can be maintained closed to this value.
2. No clogging due to salt formations.
3. Particles can be recovered in a cyclone and recycled to the reactor.
4. Particles can be easily removed and replenished with fresh catalyst if the catalyst deactivates frequently.
5. A closer control of output variables.

Kinetics of gas-solid catalyzed reactions

A realistic kinetic model for a gas-solid reaction should include the interaction of the various gas species with a solid catalyst. Hence one should consider the adsorption-desorption processes in addition to the intrinsic kinetics. Models which include these effects are known are Langmuir-Hinshelwood (L-H) models. Here we describe the methodology for the derivation of such models based on a postulated mechanistic scheme for various steps involved in the reactions. The rate limiting step hypothesis (RLS method discussed earlier) is often used to derive a final form for the kinetic model. The method is illustrated below. First we define various ways of defining the rate in these systems. Note that the general definition of the rate was given in the earlier chapter.

The general definition of rate of reaction is:

$$Rate = \frac{Number\ of\ moles\ produced\ by\ reaction}{(unit\ time)(unit\ measure\ of\ the\ system)}$$

Note that the division by unit measure of the system makes the rate an intensive property. The unit measure is simply the volume of the reactor for homogeneous system but a wide of range of choices are available for catalytic systems. The unit measure is usually some measure of the catalyst property.

Various measures are as follows:
Rate based on active metal loading
Rate based on surface (internal) area of catalyst
Rate based on the basis of unit mass of catalyst
Rate based on unit volume of catalyst

One should then be careful with the units and use appropriate conversion factors as needed.

For example rate based on unit mass of catalyst is equal to rate based on unit internal surface area multiplied by surface area per unit mass of the catalyst. The latter quantity is usually measured by Hg porosimetry and is reported as a part of catalyst specification by catalyst manufacturers.

It may be noted that the rate may not be a linear function of metal loading fro some catalyst. For example, a catalyst with 2% Pt may not show the same rate as that with 1% Pt. In some cases it does! Hence, caution should be used in converting the rate based on active metal loading to other measures shown above.

L-H Model Development

The model development is done in three steps.

- Postulation of a rate controlling step (RLS)
- Quasi-steady state or equilibrium for all the other steps
- The site balance equation for the total active sites of the catalyst

We now show the development by taking the following reaction

$A + B \rightarrow C + D$

assuming the following steps.

1. Adsorption of A and B over the active sites of the catalyst

$$A + s \rightarrow A - s \qquad (1)$$
$$B + s \rightarrow B - s \qquad (2)$$

2. Surface reaction between adsorbed A and adsorbed B. Products are on the sites.

$$A - s + B - s \rightarrow C - s + D - s \qquad (3)$$

3. Desorption of the products from the active sites. This releases the active sites for adsorption and the continuance of the catalytic cycle.

$$C - s \rightarrow C + s \qquad (4)$$
$$D - s \rightarrow D + s \qquad (5)$$

Let us develop the kinetic model assuming the surface reaction (Eq. 3) to be the rate limiting step. The rate can then be expressed as

$$(-r) = k_{s2}\left(A_s B_s - C_s D_s / K_s\right) \qquad (6)$$

where K_s is the equilibrium constant for the surface reaction (Eq.3).

All the other steps are assumed to be in equilibrium. Thus we have

$$A_s = K_A p_A [s] \qquad (7)$$

where K_A is the equilibrium constant for species A and [*s*] is the concentration of vacant sites. Similarly, for the equilibrium steps (2), (4) and (5) above we have:

$$B_s = K_B p_B [s] \quad (8)$$

$$C_s = K_C p_C [s] \quad (9)$$

$$D_s = K_D p_D [s] \quad (10)$$

Using these in Eq. (6) leads to

$$(-r) = k_{s2}[s]^2 (K_A K_B p_A p_B - K_C K_D p_C p_D / K_s) \quad (11)$$

This is rearranged to:

$$(-r) = k_{s2} K_A K_B [s]^2 (p_A p_B - p_C p_D (K_C K_D / K_A K_B K_s)) \quad (12)$$

Since the catalyst does not affect the equilibrium constant for the overall reaction the last bracketed term in the above equation is the equilibrium constant for the reaction (based on gas phase partial pressures):

$$K_{eq} = K_A K_B K_s / K_C K_D \quad (13)$$

Hence Eq. (12) can be expressed as

$$(-r) = k_{s2} K_A K_B [s]^2 (p_A p_B - p_C p_D / K_{eq}) \quad (14)$$

The final step is to obtain an expression for the concentration of vacant sites [*s*]. Let the total concentration of sites (occupied plus vacant) be S_0. Then a site balance leads to:

$$S_0 = [s] + A_s + B_s + C_s + D_s \quad (15)$$

Using the equations for A_s etc and rearranging

$$[s] = S_0 / (1 + K_A p_A + K_B p_B + K_C p_C + K_D p_D) \quad (16)$$

Using this in Eq (14) we obtain:

$$(-r) = \frac{k_{s2} K_A K_B S_0^2 (p_A p_B - p_C p_D / K_{eq})}{(1 + K_A p_A + K_B p_B + K_C p_C + K_D p_D)^2} \quad (17)$$

Usually the total concentration of sites is difficult to measure and hence this term is absorbed with the rate constant k_{s2}. Thus defining $k_s = k_{s2} S_0^2$ we obtain

$$(-r) = \frac{k_s K_A K_B \left(p_A p_B - p_C p_D / K_{eq}\right)}{\left(1 + K_A p_A + K_B p_B + K_C p_C + K_D p_D\right)^2} \qquad (18)$$

which is the L-H model for a surface reaction controlling process.

Some common L-H type of rate models together with the postulated rate controlling steps are below: For simplicity of presentation, the reactions are considered irreversible, i.e. K_{eq} is set as ∞.

1. Adsorption of A rate limiting: other species weakly absorbed.

$$(-r) = \frac{k_1 S_0 p_A}{\left(1 + K_A p_A\right)} \qquad (19)$$

2. Dissociative adsorption of A; surface reaction controls
Here the adsorption step is represented as:

$$A_2 + 2s \rightarrow 2A - s$$

and this type of mechanism is common for species such as H2 adsorbing on noble metals. Reaction is represented for simplicity as:

$$2A - s \rightarrow \text{Pr}\,oducts + 2s$$

This leads to the following rate expression:

$$(-r) = \frac{k_1 s_{01} p_A}{\left(1 + K_A \sqrt{p_A}\right)^2} \qquad (20)$$

and this rate model has been shown to be useful to represent the kinetics of some hydrogenation reactions.

3. A and B adsorbed on separate sites: surface reaction controls the process.

$$(-r) = \frac{k_1 s_{01} s_{02} p_A p_B}{\left(1 + K_A p_A\right)\left(1 + K_B p_B\right)} \qquad (21)$$

4. Reaction of adsorbed A with gas phase B. (B need not be adsorbed for reaction to occur.) Surface reaction controlling

$$(-r) = \frac{k_s K_A \left(p_A p_B\right)}{\left(1 + K_A p_A + K_C p_C + + K_D p_D\right)} \qquad (22)$$

Note that the denominator is to the power one now representing the fact that this is a single site mechanism. $K_C = K_D = 0$ if products are not adsorbed. A model of this type is used in selective catalytic reduction.

Power law vs L-H Models

Characteristics of the L-H can be examined by considering a simple case. Assume that only the species A is strongly adsorbed and the reaction is irreversible. Assume B is in excess and a dual site mechanism. This leads to the following simplified rate model:

$$(-r) = \frac{k_s K_A p_A}{(1 + K_A p_A)^2} \qquad (23)$$

The rate constant k_s increases with temperature while the adsorption equilibrium constant K_A generally decreases with temperature. The net effect may be such that the rate reaches a maximum at a particular temperature. This can not be predicted by power law model. Another observation is the dependency on concentration. For low concentration, the reaction would be seen as a first order while for high concentration, a negative first order dependency may be observed.

For other complex schemes, the rate can reach a maximum at an intermediate coverage of, say *B*, in a bimolecular reaction *A*+*B* to products. The advantage of the power law models are their simplicity. This is especially useful if one needs to include the transport effects and use them in a reactor model. Also simple power law models are often found to fit the data well even for the case where L-H models have been fitted. Two different mechanisms L-H may produce similar rate models and model discrimination can often be difficult.

Microkinetic Models

The model is built using elementary reactions that occur on the catalytic surface and their relation with each other and with the surface during the catalytic cycle. The major advantage is implementation of surface bonding and correlation of surface structure with semiempirical molecular interaction parameters. Another advantage is that the rate constants for similar types of reaction can be estimated by molecular considerations and extrapolated to a wider class of similar types of reactions. Rate constants for individual elementary reactions can be measured independently and these can be used in the overall scheme. One limitation of this approach is that the rate expressions cannot be often obtained analytically. Numerical solutions are needed but the resulting equations are often stiff due to the wide range of time constants for the various elementary steps.

An example of a microkinetic model for catalytic oxidation in a three way converter (TWC) is shown in Table 1 from the work of Koci et al. The catalyst was $Pt/Ce/\gamma\text{-}Al_2O_3$ and the process involves CO oxidation, hydrocarbon oxidation and NO_x

reduction. (Hence the terminology three way converter). The scheme is illustrative of the complex multi-step nature of catalytic process.

Table 1
Microkinetic reaction scheme used in the model of TWC

No.	Reaction step	Kinetic expression
1	$CO + * \rightleftharpoons CO^*$	$R_1 = k_1^f L_{NM} c_{CO}^s \theta_* - k_1^b L_{NM} \theta_{CO^*}$
2	$O_2 + 2* \rightarrow 2O^*$	$R_2 = k_2 L_{NM} c_{O_2}^s \theta_*$
3	$CO^* + O^* \rightarrow CO_2 + 2*$	$R_3 = k_3 L_{NM} \theta_{CO^*} \theta_{O^*}$
4	$CO + O^* \rightleftharpoons OCO^*$	$R_4 = k_4^f L_{NM} c_{CO}^s \theta_{O^*} - k_4^b L_{NM} \theta_{OCO^*}$
5	$OCO^* \rightarrow CO_2 + *$	$R_5 = k_5 L_{NM} \theta_{OCO^*}$
6	$C_2H_2 + * \rightleftharpoons C_2H_2^*$	$R_6 = k_6^f L_{NM} c_{C_2H_2}^s \theta_* - k_6^b L_{NM} \theta_{C_2H_2^*}$
7	$C_2H_2^* + 2* \rightleftharpoons C_2H_2^{**}$	$R_7 = k_7^f L_{NM} \theta_{C_2H_2^*} \theta_*^2 - k_7^b L_{NM} \theta_{C_2H_2^{**}}$
8	$C_2H_2^* + 3O^* \rightarrow 2CO^* + H_2O + 2*$	$R_8 = k_8 L_{NM} \theta_{C_2H_2^*} \theta_{O^*}$
9	$C_2H_2^{**} + 3O^* \rightarrow 2CO^* + H_2O + 4*$	$R_9 = k_9 L_{NM} \theta_{C_2H_2^{**}} \theta_{O^*}$
10	$C_2H_2 + O^* \rightleftharpoons C_2H_2O^*$	$R_{10} = k_{10}^f L_{NM} c_{C_2H_2}^s \theta_{O^*} - k_{10}^b L_{NM} \theta_{C_2H_2O^*}$
11	$C_2H_2O^* + 2O^* \rightarrow 2CO^* + H_2O + *$	$R_{11} = k_{11} L_{NM} \theta_{C_2H_2O^*} \theta_{O^*}$
12	$O_2 + 2s \rightarrow 2O^s$	$R_{12} = k_{12} L_{OSC} c_{O_2}^s \zeta_s$
13	$CO^* + O^s \rightarrow CO_2 + * + s$	$R_{13} = k_{13} L_{NM} \theta_{CO^*} \zeta_{O^s}$
14	$C_2H_2^* + 3O^s + * \rightarrow 2CO^* + H_2O + 3s$	$R_{14} = k_{14} L_{NM} \theta_{C_2H_2^*} \zeta_{O^s}$
15	$CO_2 + \gamma \rightleftharpoons CO_2^\gamma$	$R_{15} = k_{15}^f L_{SUP} c_{CO_2}^s Z_\gamma - k_{15}^b L_{SUP} Z_{CO_2^\gamma}$
16	$NO + * \rightleftharpoons NO^*$	$R_{16} = k_{16}^f L_{NM} c_{NO}^s \theta_* - k_{16}^b L_{NM} \theta_{NO^*}$
17	$NO^* + * \rightarrow N^* + O^*$	$R_{17} = k_{17} L_{NM} \theta_{NO^*} \theta_*$
18	$NO^* + N^* \rightarrow N_2O^* + *$	$R_{18} = k_{18} L_{NM} \theta_{NO^*} \theta_{N^*}$
19	$N_2O^* \rightarrow N_2O + *$	$R_{19} = k_{19} L_{NM} \theta_{N_2O^*}$
20	$N_2O^* \rightarrow N_2 + O^*$	$R_{20} = k_{20} L_{NM} \theta_{N_2O^*}$
21	$N^* + N^* \rightarrow N_2 + 2*$	$R_{21} = k_{21} L_{NM} \theta_{N^*}^2$
22	$NO + O^* \rightleftharpoons NO_2^*$	$R_{22} = k_{22}^f L_{NM} c_{NO}^s \theta_{O^*} - k_{22}^b L_{NM} \theta_{NO_2^*}$
23	$NO_2^* \rightleftharpoons NO_2 + *$	$R_{23} = k_{23}^f L_{NM} \theta_{NO_2^*} - k_{23}^b L_{NM} c_{NO_2}^s \theta_*$

The reaction subsystems for CO and C_2H_2 oxidation on noble metal (*), O_2 storage and release on ceria (s), CO_2 storage on γ-Al_2O_3 (γ) and NO_x transformation on noble metal (*) are separated by blank lines. For values of the kinetic parameters cf. Nibbelke et al. (1998), Harmsen et al. (2001a,b), and Mukadi and Hayes (2002).

Surface Interaction Models

Experimental methods, namely NMR, spectroscopy, and kinetic measurements are available to study the surface topology of catalysts, the adsorption sites and how the molecules are adsorbed on the catalyst surface. Unfortunately these experiments are very difficult to perform and most of the time, there is a high discrepancy between different techniques. Computer simulations, therefore are becoming increasingly popular to study the structure and the transport behavior of the catalysts.

The two commonly used simulation techniques to study the structural and dynamical properties include Molecular Dynamics (MD) and Monte Carlo (MC) simulations. MD has been extensively used to study dynamic and equilibrium properties of different adsorbates in different catalysts. In MD simulation, Newton's equations of motion are solved for each molecule. Since the continuous motion of the molecules is approximated by discrete movements in time, MD simulations are deterministic. The time step used in the calculations is usually between 5-10 fs resulting in practical simulation times up to 10 ns with current computers. MC simulation, on the other hand is a probabilistic method. Many useful information such as energetics of the individual adsorption sites, adsorption isotherms and related thermodynamic properties properties can be obtained by MC simulations. More information about these techniques can be found at [1].

MC simulations are also used to study surface reactions. Much effort has been focused on study of reduction reaction of NO by CO since this is a very important reaction in pollution control in catalytic converters. This reaction is very sensitive to the metal substrate used as a catalyst and to the type of the surface[3]. The MC algorithm involves randomly selecting an event from the given mechanism with a probability based on the reaction rate constants. Usually 10^6 MC steps are attempted to reach stability in the results. Cortes et al [2] studied this reaction over the Rh catalyst. The authors found that there is a good agreement between the MC simulations and the analytical solutions of Langmuir-Hinshelwood mechanism. Korluke et al [3] developed a simple lattice gas model to study the effect of molecularly adsorbed NO using MC simulations. The authors found that NO and CO desorption is necessary for a steady-state reaction.

The problem with these simulations is that the texture of the porous catalyst might be too complex for realistic representation. Many simplifications are made in the modeling. Still, the simulations provide a lot of information about the surface reactions, and structure and properties of surfaces. Simulation results can be used in microkinetic model which can then be used to construct more realistic L-H models. Thus the three modes together provide a hierarchy for multi-scale analysis.

Kinetic Model: Examples

1. SCR

   A mechanism proposed is adsorption of NH3 on active sites followed by reaction with NO in the gas phase.

$$NH_{3(g)} + s \underset{k_b}{\overset{k_f}{\leftrightarrow}} NH_3 s \qquad K = k_f / k_b$$

$$NH_3 s + NO(g) + \frac{1}{4} O_2 \xrightarrow{k} N_2 + \frac{6}{4} H_2 O$$

Step 2 is assumed to be rate controlling. Then

$$r = k(NH_3 s)(NO)$$
$$NH_3 s = K(NH_3)_g (s)$$

Rate is therefore equal to $kK(NO)_g (NH_3)_g s$

A site balance gives

$s + NH_3 s = s_0$ or

$$s + K(NH_3)_g s = s_0$$

$$s = \frac{s_0}{(1 + K(NH_3)_g)}$$

Hence the proposed kinetic scheme is

$$r = \frac{s_0 kK(NO)_g (NH_3)_g}{1 + K(NH_3)_g}$$

Reaction Engineering Issues

In this section, we indicate the main reaction engineering problems associated with gas-solid reaction. The modeling tasks can be divided into two categories:

i. Particle scale modeling

Since the catalyst is generally porous, intraparticle diffusion becomes an important rate limiting factor. Thus, one needs to consider the diffusion in the pores of the catalyst with simultaneous chemical reaction. In case of monolithic type of catalyst, particle scale modeling is replaced by modeling of surface adsorption, desorption and reaction processes.

ii. Reactor scale modeling

The reactor scale modeling consists of writing the mass and heat balances for the reactor including flow non-idealities, if any. The particle scale model becomes a sub-model here and provides the necessary expressions for the rate of reaction.

Reactor Models Coupling with Particle Models:

In order to see the coupling of reactor models with particle model it is useful to consider a packed bed reactor which is modeled as a plug flow reactor. Also isothermal conditions are considered first. Consider a differential element of reactor change in molar flow rate if *I* is given as:

$$\Delta F_i = R_i \times (measure\, used\, to\, define\, rate)$$

A mass balance leads to:

$$\frac{dN_i}{dx} = (1-\varepsilon_B)R_i = \sum v_{ji} r_j$$

Also

$$N_i = N_t y_i$$

$$N_t = \frac{PQ_G}{RT}$$

where R_i is the rate of production of species *i* per unit catalyst volume. Hence the factor $(1-\varepsilon_B)$ appears in the rate term on RHS. Since $N_i = u_g c_{gi}$ the equation can be written as:

$$u_g \frac{dc_{g,i}}{dx} + c_{g,i} \frac{du_g}{dx} = (1-\varepsilon_B)R_i$$

If change in the gas velocity is small (e.g. dilute systems) then

$$u_g \frac{dc_{g,i}}{dx} = (1-\varepsilon_B)R_i = (1-\varepsilon_B)\sum v_{ji} r_j$$

For single reactions

$$R_i = v_i r$$

and *r* depends on the conditions in the catalyst. The rate based on c_{gi} would not in many cases be a representative estimate of the rate at a given location in the reactor. This is due to transport limitations which leads to a concentration variation across the gas film and in the pores of the catalyst. A typical concentration variation is shown in Figure 4

and the role of the particle scale models is to take into account these variations to find a representative rate.

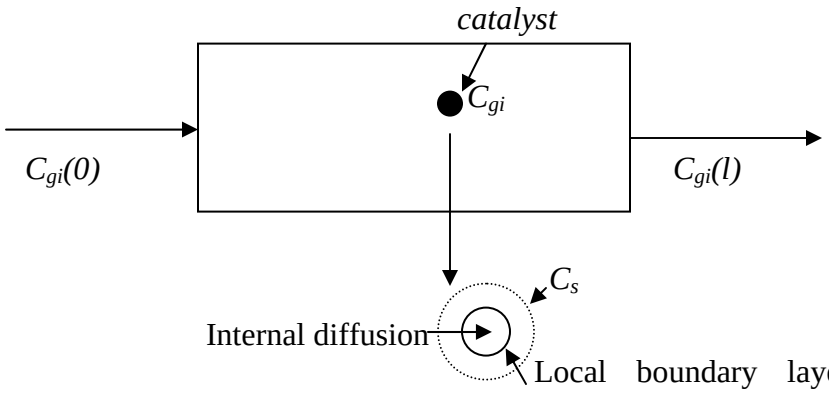

Note that similar profiles exist for temperature.

For single reaction and dilute systems, we have the following equation for each species *i*.

$$u_g \frac{dc_{g,i}}{dx} = (1-\varepsilon_B)R_i = (1-\varepsilon_B)\nu_i r \qquad (1)$$

r = rate of reaction including transport effects, i.e. including the effect of point to point variation of concentration in the catalyst.
Let $\sim r(c_{g,i}, T_g)$ be the rate based on bulk conditions. Ratio of r to $\tilde{r}$ is called effectiveness factor and is of great convenience in modeling heterogeneous systems.
Eq. 1 becomes

$$u_g \frac{dc_{g,i}}{dx} = (1-\varepsilon_B)\nu_i r(c_{g,i}, T_g)\eta \qquad (2)$$

In general, η is a function of $c_{g,i}$ and T_g. Only for first order isothermal case η can be found independently as shown later.

Solution of Eq. (2) is done numerically for multiple species and multiple reactions. The procedure is similar to that homogeneous reactions with a major difference that at each integration step η_0 need to be computed by a "particle model" based on the local values of gas phase concentrations and temperatures.

Particle models are considered in detail in the following section.

Particle Models

1. **Models for internal diffusion**

The particle scale effects are usually modeled by the diffusion-reaction equation. More detailed models using Stefan-Boltzmann equations are not considered here. The diffusion in a porous catalyst is characterized by an effective diffusivity, $D_{e,i}$ with i indicating the species. The transport of species i within the pore structure is then governed by the following equation for a spherical catalyst

$$D_{ei}\nabla^2 C_i = \sum \upsilon_{ji}\left(-r_j\right)a_j(r)r_j + 0 < r < R \tag{1}$$

where the quantities used are defined as follows:

∇^2 = Laplacian which takes the following form for a spherical catalyst.

∇^2 = $\frac{1}{r^2}\frac{\partial}{\partial r}r^2\frac{\partial}{\partial r}$

r = Radial position

R = Radius of the catalyst

$D_{e,i}$ = Effective diffusivity of species i in the pores of the catalyst; Model assumes the same diffusivity for the poisoned and unpoisoned zones.

υ_{ji} = Stoichiometric coefficient of species i in the j-th reaction

r_j = rate expression of j-th reaction per unit total volume of catalyst.

$a_j(r)$ = Activity of the catalyst for the j-th reaction; Note the radial dependence of the activity profile. This quantity may change with time as the catalyst gets progressively poisoned.

The boundary conditions needed to solve Eq. (1) are as follows:

$$\text{at } r = 0, \quad \frac{\partial C_i}{\partial r} = 0 \tag{2}$$

$$\text{at } r = R, \quad \frac{\partial C_i}{\partial r} = \frac{k_{g,i}}{D_{e,i}}\left(C_{g,i} - C_i\right) \tag{3}$$

where $k_{g,i}$ is the gas film mass transfer coefficient for the i-th species.

$C_{g,i}$ = concentration of species i in the external gas phase near the particle under consideration. Again $k_{g,i}$ is based on concentration driving force. Various definitions are used for k_g and units should be used carefully. The solution of Eq.(1) gives the detailed concentration profiles in the particles. From the solution, an average rate can be calculated and used to find η_0. This forms the basis for the particle model.

First Order Reaction

The intraparticle diffusion models simplify for a first order kinetics. For this case, the results can be obtained analytically. The first order kinetics is often a good approximation in oxidation reactions. The oxygen is usually present in excess compared to the pollutants. For such cases, the kinetics can be simplified to a first order kinetics:

$$r_j = k_j\, C_j$$

where r_i refers to the oxidation of the i-th pollutants and k_j to the corresponding rate constant. Further, if one assumes that the activity of the catalyst is uniform (a starting assumption) then the following equation holds for species *i*:

$$D_{ei}\, \nabla^2\, C_i = k\, C_i \qquad (4)$$

where k = rate constant for reaction of species *i* (now $k = k_i$ here). Note that k is based on unit volume of the catalyst.
The characteristic dimensionless groups which govern the process are as follows:

1. Thiele modulus, $\phi^2 = \dfrac{k\, R^2}{D_{ei}}$

   This arises from the normalization of the governing differential equation. (Eq(4))

2. Biot number for mass transfer

$$Bi_M = \frac{k_g R}{D_e}$$

   This arises from the normalization of the boundary conditions.

The solution of Eq. (4) can then be represented as:

$$c = \frac{C_i}{C_{g,i}} = \left[\frac{Bi_M}{\phi\, Coth\, \phi - 1 + Bi_M}\right] \frac{\sinh \phi\, \xi}{\xi \sinh \phi}$$

where ξ is the dimensionless radial position = $\dfrac{r}{R}$. Also note that

$\dfrac{C_{i_1} s}{C_{g,i}} = \left[\dfrac{Bi_M}{\phi\, Coth\, \phi - 1 + Bi_M}\right]$ by setting ξ =1. This gives the drop in the gas film for C.

Here $C_{i_1} s$ = concentration at the catalyst surface.

The effect of intraparticle diffusion is expressed conveniently in terms of the effectiveness factor for the catalyst. This factor is defined as the actual rate of reaction over the entire catalyst divided by the maximum rate of reaction.

Actual rate of reaction = $\int_o^R 4\pi\, r^2\, k\, C\, dr$

Maximum rate of reaction = $\frac{4}{3}\pi R^3 k C_g$

Note the species subscript, *i*, has been dropped for convenience.

The actual rate of reaction can also be expressed as:

Actual Rate $= 4\pi R^2 D_e \left(\frac{\partial C}{\partial r}\right)_{n=R}$ which is a simpler form to calculate.

The expression for the overall effectiveness factor η_o is then obtained as:

$$\eta = \frac{3}{\phi^2}(\phi \coth \phi - 1)\frac{Bi_M}{(\phi \coth \phi - 1 + Bi_M)}$$

Also the following limiting case when $Bi_M \to \infty$ should be noted

$\eta_c = \frac{3}{\phi^2}(\phi \coth \phi - 1)$ which is also referred to as the internal effectiveness factor.

The above expression is suitable for a spherical catalyst. For catalyst of other shapes it is convenient to use a "shape normalized" Thiele modulus defined as

$$\Lambda = \frac{V_p}{S_p}\left(\frac{k}{D_e}\right)^{1/2}$$

where V_p is the volume of the catalyst and S_p is the external surface area of the catalyst. Note that $\Lambda = \frac{\phi}{3}$ for a sphere.

An approximate expression for effectiveness factor for all shapes is given by:

$$\eta_c \approx \frac{\tanh \Lambda}{\Lambda}$$

This is based on a slab model for geometry of the catalyst assuming there is no gas side resistance. In the limit of large Λ, we can use η as the reciprocal of Λ since the $\tanh \Lambda \to 1$ for large Λ. The concentration profiles in a slab catalyst for various values of Λ is shown in Figure 5.

FIGURE MISSING

Application problems to ascertain the importance of pore diffusion are illustrated by the following examples.

Problem 1: Rate for larger size given kinetics

Rate of reaction over a finely crushed catalyst of radius of 0.5mm was measured as 10.0 mole/sm^{3}catalyst.

Temperature is 400 K and pressure is 10^5 Pa and mole fraction of reactant in the gas is 0.1. Find the rate for a catalyst of pellet radius of 3mm.

Solution:
Assume ηc=1 for small catalyst.

$$C_{Ag} = \frac{yP}{RT} = \frac{0.1\times 10^5}{8.314\times 400} = 3.007\frac{mol}{m^3}$$

$$Rate = kC_{Ag} \text{ Hence } k = \frac{Rate}{C_{Ag}} \quad k = \frac{10\, mol/m^3 s}{3.007\, mol/m^3} = 3.3256\, s$$

To find rate for larger catalyst, we need an estimate of intraparticle diffusion coefficient. Let D_e = 4x10^{-6} m^2/s (a reasonable estimate). Then,

$$\phi = \frac{R}{3}\sqrt{\frac{k}{D_e}} = 0.9118$$

$$\eta_c = 0.7051$$

$$Rate = \eta_c k C_{Ag} = 7.05\, mole/m^3 s$$

Diagnostics: The Weisz Model
Given the measured rate, establish if there is significant pore diffusion resistance.

$$M_W = Weisz\, Modulus = \frac{L^2(-R_A)_{obs}}{C_{Ag}D_e}$$

where $L = R/3$ = characteristic length scale

If Weisz modulus (Wagner modules) < 0.15, then the concentration profile in the pellet is nearly uniform.

Note that

$$M_W = \eta_c \phi^2$$

Problem 2: Test for pore resistance
A rate of 10^5 mole/hr m^3 cat is observed for a gas concentration of A of 20 mole/m^3. The catalyst particle diameter is 2.4 mm.

An independently measured value is needed to solve this problem.
Let us assume effective diffusivity is 5×10^{-5} m^2/hr.

Is there a strong pore diffusion resistance?

Solution:
L = R / 3 = 4 x 10^{-4} mm

Wagner modulus =

$$M_T = \frac{L^2(-R_A)_{obs}}{D_e C_{Ag}} = 16$$

Strong pore resistance

The measured data are not representative of true or "intrinsic" kinetics.

Problem 3: Intrinsic kinetics
In Problem 2, find the effectiveness factor and the true rate constant.

Solution:

$$rate = k\eta C_{Ag}$$

$$k\eta = \frac{rate}{C_{Ag}} = 5000 hr^{-1}$$

Since h depends on *k*, we used a trial and error solution. We expect h to be small. Let us assume some value, say 0.01.

Then

$$k_V = \frac{5000}{\eta} = 5 \times 10^5$$

$$Thiele\,\mathrm{mod}\,ulus = L\sqrt{\frac{k_V}{D_e}} = 40$$

$$\eta = \frac{\tanh\phi}{\phi} = 0.025$$

η assumed	$k_v=5000/\eta$	Thiele	η equation
0.01	5x105	40	0.025
0.03	1.67x105	23	0.0433
0.063	7.93x104	15.9	0.0627

Design Considerations Monolith Models

Gas phase balance

$$Q_G \Delta c_{gi} = v_i r \Omega \Delta V$$

where r = rate of reaction, single reaction case
Ω = measure used to define the rate per unit reactor volume

For multiple reactions, $v_i r$ is replaced by $\sum v_{ji} r_j$ where j is the reaction index.

Wash-coat case
r based on external surface area of the walls of the monolith
Ω = surface area per unit volume of monolith
$\Delta V = A_c \Delta x$
A_c = cross sectional or frontal area

$\frac{Q_L}{A_c} = u_g$ = gas superficial velocity

$$u_g \frac{dc_{gi}}{dx} = v_i r \Omega$$

If r is based on bulk concentration we have the pseudo-homogeneous model. If r is based on actual concentration, use effectiveness factor

$$u_g \frac{dc_{gi}}{dx} = v_i \eta r\left(c_{g1},...,c_{gL}\right)\Omega$$

To find η, balance transport to surface and reaction at the surface.

$k_{mi}\left(c_{gi} - c_{si}\right) = -v_i r\left(c_{si}\right)$ for each species. (A)
Solve for c_{si}. Find $r(c_{si})$.

$$\eta = \frac{r\left(c_{si}\right)}{r\left(c_{gi}\right)}$$

Note that k_m varies with x in laminar flow. Hence these calculations are to be repeated for each incremental position in x.

Alternate formulation is in terms of transfer rate to the walls. (similar to that in Wendt's paper) Here η is not explicitly calculated. Both c_{gi} and c_{si} are treated as variables. We will look at this formulation now.

Gas phase balance

$Q_G \Delta c_{gi}$ = - transferred to walls = $-k_{mi}\Omega\Delta V\left(c_{gi}-c_{si}\right)$

where Ω = surface area of the walls per unit reactor volume

$$u_g \frac{dc_{gi}}{dx} = -\Omega k_{mi}\left(c_{gi}-c_{si}\right) \text{ for } i = 1 \text{ to N}$$

$$k_{mi}\left(c_{gi}-c_{si}\right) = -\nu_i r\left(c_{si}\right)$$

Both of these equations are solved simultaneously. Note that this is a differential algebraic system. Both methods are equivalent.

Computation of η is simple for a first order reaction. Here Eqn. (A) reduces to

$$k_{mi}\left(c_{gi}-c_{si}\right) = r\left(c_{si}\right) = k\, c_{si} \qquad \text{(B)}$$

where ν_i is taken as –1 for the key reactant. Eliminating c_{si}

$$r = c_{gi}\left[\frac{1}{k_{mi}}+\frac{1}{k_{si}}\right]^{-1}$$

$$r_{actual} = c_{gi}\frac{k_{mi}k_{si}}{k_{mi}+k_{si}}$$

$$\eta = \frac{k_{mi}}{k_{mi}+k_{si}}$$

The reactors are operated often in laminar flow. The transfer coefficient k_{mi} can then be predicted by detailed 2-D models for diffusion and flow.

Calculation of η for two components reacting with each other is slightly complicated. Eqn. (B) is now written for both components.

$k_{m1}\left(c_{g1}-c_{s1}\right) = -\nu_1 k_2 c_{s1} c_{s2}$ or other rate form

$k_{m2}\left(c_{g2}-c_{s2}\right) = -\nu_2 k_2 c_{s1} c_{s2}$

$$\eta = \frac{c_{s1}c_{s2}}{c_{g1}c_{g2}}$$

Equations have to be solved simultaneously for c_{s1} and c_{s2}. Then η can be computed. Note that η varies along the reactor since the concentrations c_{s1} and c_{s2} also vary along

the reactor axial position. The calculation procedure for local values of η is illustrated in the following example.

Example: Consider a bimolecular reaction.

$NO_x + vNH_3 \rightarrow products$

where $v = 2/3\ x$

This is representative of SCR. Rate of transport of NO_x (denoted as species 1) is:

$$r = k_{m1}\left(c_{1g} - c_{1s}\right)$$

$$c_{1g} - c_{1s} = \frac{r}{k_{m1}}$$

$$c_{1s} = c_{1g} - \frac{r}{k_{m1}}$$

Rate of transport of NH3 is:

$$vr = k_{m2}\left(c_{2g} - c_{2s}\right)$$

$$c_{2g} - c_{2s} = \frac{vr}{k_{m2}}$$

$$c_{2s} = c_{2g} - \frac{vr}{k_{m2}}$$

Rate of reaction is $r = k_{s2}c_{1s}c_{2s}$

$$r = k_{s2}\left(c_{1g} - \frac{r}{k_{m1}}\right)\left(c_{2g} - \frac{r}{k_{m2}}\right)$$

Rate is often expressed in terms of an effectiveness factor

$$r = k_{s2}c_{1g}c_{2g}\eta$$

Substituting and rearranging, an expression for η is obtained:

$$\eta = \left(1 - \frac{k_{s2}c_{2g}\eta}{k_{m1}}\right)\left(1 - \frac{vk_{s2}c_{1g}\eta}{k_{m2}}\right)$$

The effectiveness factor is now a function of local gas phase concentration.

Design Parameters

1. Binary Diffusivity in Gas Phase.

Binary diffusion coefficient for a pair of gases denoted as 1 and 2 can be calculated by using Lennard-Jones potential model. The equation suggested by Hirschfelder, Bird and Spotz is:

$$D_{12} = D_{21} = \frac{1.86 \times 10^{-7}\ T^{3/2} \sqrt{\frac{1}{M_1} + \frac{1}{M_2}}}{\sigma_{12}^{\ 2}\ \Omega_D\ P}$$

where T is the absolute temperature, P is the absolute pressure in atm, M_1 and M_2 are the molecular weights. The two Lennard-Jones parameters are σ_{12} the collision diameter in angstroms and Ω_D the collision integral for diffusion. These values are usually tabulated. The quantity σ_{12} is calculated as the average:

$$\sigma_{12} = \frac{1}{2}(\sigma_1 + \sigma_2)$$

The collision integrals are function of a parameter $\frac{kT}{\varepsilon}$. This is calculated from the values of ε_1 and ε_2 for each gases as:

$$\frac{\varepsilon_{12}}{k} = \sqrt{\frac{\varepsilon_1}{k}\frac{\varepsilon_2}{k}}$$

NOTE: k = Boltzmann constant

Example: Estimate diffusion coefficient of CO in air at 800k and 1 atm.

From the tables of Lennard-Jones force constants we find the following values:

	ε/k in K ,	σ in A
Air	97	3.617
CO	110	3.590

$$\sigma_{12} = \frac{1}{2}(\sigma_1 + \sigma_2) = 3.6035$$

$$\frac{\varepsilon_{12}}{k} = \sqrt{(97)(110)} = 103.29$$

$$\frac{k}{\varepsilon_{12}}T = \frac{800}{103.29} = 7.745$$

From the table of collision integrals, the value of Ω_D is 0.77.

Substituting into the formula

$$D_{12} = \frac{1.86\times10^{-7}\times(800)^{3/2}\left(\frac{1}{28}+\frac{1}{29}\right)^{1/2}}{(3.6035^2)(0.77)(1)}$$
$$= 1.1\times10^{-4}\ m^2/s$$

---

2. EFFECTIVE DIFFUSION COEFFICIENT

The diffusion within the catalyst proceed by two mechanisms: (1) Bulk diffusion within the pores(2) bombardment with the walls of the pore if the pore radius is small. The second mechanism is know as Knudsen diffusion.

The bulk phase diffusivity is corrected for internal pore diffusion by incorporating two factors (1) porosity, ε which accounts for the reduced area accessible for diffusion and (2) tortuosity, τ which accounts for the non-straight path for diffusion.

$$D_{12,eff} = D_{12}\frac{\varepsilon}{\tau}$$

The Knudsen diffusion coefficient depends on the average radius of the pores and is given by:

$$D_{K,eff} = \frac{\varepsilon}{\tau}D_K$$

Where D_K is the Knudsen diffusivity in a single cylindrical pore.

Knudsen diffusion occurs when the size is the pores of the order of mean free path of the diffusivity molecule.

where D_K is the Knudsen diffusion coefficient given as:

$$D_K = \frac{2}{3}r_e V_1$$

r_e = effective pore radius and V_1 is the average molecular speed of species 1. This is given by:

$$V_1 = \left(\frac{8RT}{\pi M_1}\right)^{1/2}$$

Substituting the values of gas constants, we find the following dimensional equation for the Knudsen diffusion coefficient.

$$D_{K,1} = 97\, r_e \left(\frac{T}{M_1} \right)^{1/2}$$

in m^2/s with r_e in m and T in Kelvins.

The phenomena of ordinary diffusion and Knudsen diffusion, may be occurring simultaneously. The two can be combined by the following formula:

$$\frac{1}{D_{1,eff}} = \frac{1}{D_{12,eff}} + \frac{1}{D_{K,eff}}$$

Additional mechanism is the surface diffusion where the adsorbed species migrates along the surface. The effects are often ignored if the pores are relatively large. This phenomena may be of importance in monolith type of catalysts.

EXAMPLE:

Calculate the effective diffusivity of CO in porous alumina catalyst whose physical characteristics are as follows: Porosity = 0.8. Average pore diameter = 1 μm.

$$D_{12,eff} = \frac{\varepsilon_v}{\tau} D_{12} = \frac{0.8}{4.0} \left(1.06 \times 10^{-4}\right) = 2.12 \times 10^{-5}\ m^2/s$$

where D_{12} is taken as the value for a CO-air mixture at 800 K, 1 atm.

$$\begin{aligned}
D_{K1,eff} &= \frac{2}{3} \frac{\varepsilon_v}{\tau} r_e\, \bar{v}_1 \\
r_e &= 1\ \mu m = 10^{-6}\ m \\
\bar{v} &= \left(\frac{8RT}{\pi M_1} \right)^{1/2} \\
&= \left\{ \frac{(8)\left(8.314 \times 10^3\ J/kmol\ K\right)(800\ K)(1\ N\ m/J)\left(1\ kg\ m\ s^{-2}/N\right)}{(\pi)(28\ kg/kmol)} \right\}^{1/2} = 778\ m/s \\
D_{K1,eff} &= \frac{2}{3}(0.8/4.0)\left(10^{-6}\ m\right)(778\ m/s) = 1.04 \times 10^{-4}\ m^2/s
\end{aligned}$$

Then, the effective diffusion coefficient is:

$$\begin{aligned}
\frac{1}{D_{1,eff}} &= \frac{1}{D_{12,eff}} + \frac{1}{D_{K1,eff}} = \frac{1}{2.12 \times 10^{-5}} + \frac{1}{1.04 \times 10^{-4}} \\
D_{1,eff} &= 1.76 \times 10^{-5}\ m^2/s
\end{aligned}$$

GAS SIDE MASS TRANSFER COEFFICIENT

The external mass transfer coefficient from a spherical particle is correlated by the following dimensionless equation

$$Sh = 2 + 0.69\ Re^{1/2}\ Sc^{1/3}$$

where

Sh = Sherwood number = $\frac{k_g}{D}\ d_p$

Re = Reynolds number = $\frac{U_g}{\upsilon}\ d_p$

U_g is the linear velocity of the gas on the bulk stream.

Sc = Schmidt number = $\frac{\upsilon}{D}$

The corresponding value for the heat transfer coefficient can be obtained by using the analogy between heat and mass transfer. The above correlation can be used for heat transfer with Nusselt and Prandtl number substituting the Sherwood and Schmidt terms.

An alternate correlation recommended by Whitaker is:

$$Nu = 2 + \left(0.4\ Re^{1/2} + 0.06\ Re^{2/3}\right) Pr^{0.4}$$

INTERNAL FLOW

Mass and heat transfer coefficient for flow through internal ducts are needed for the design of monolith catalysts. For this case the correlation for laminar flow in a circular pipe is used but the channel diameter is replaced by the equivalent hydraulic diameter. For pipe flow, the following correlation is useful for laminar flow

$$Nu = 3.66 + \frac{0.065\left(D/L\right)\mathrm{Re\ Pr}}{1 + 0.04\left[\frac{D}{L}\mathrm{Re\ Pr}\right]^{2/3}}$$

Equation is valid for Re < 2300 and assuming a constant wall temperature.

Note that the *Nu* reaches the asymptotic value of 3.66. The thermal entry length (a point at which the Nusselt number reaches the asymptotic value) is given by the following expression.

$$\frac{L_{eh}}{D} = 0.017\ Re\ Pr$$

For other geometry the concept of hydraulic diameter can be used.

$$\text{Hydraulic diameter} = 4 \cdot \frac{\text{Area of cross section}}{\text{Wetted perimeter}}$$

The asymptotic Nusselts number for various geometries are shown below:

TABLE 2: Nusselt numbers and the product of friction factor times Reynolds number for fully developed laminar flow in ducts of various cross-sections.

	Nu_{D_h}		
Cross Section	**Constant Axial Wall Heat Flux**	**Constant Axial Wall Temperature**	$f\ Re_{D_h}$
Equilateral Triangle	3.1	2.4	53
Circle	4.364	3.657	64
1 Square 1	3.6	2.976	57
∞	8.235	7.541	96

An example problem to estimate the effect of mass transfer in monolith arrangement is given below.

EXAMPLE

A reactor walls consist of passages which are square in cross section with 1 mm sides. The walls are coated with a catalyst which oxidizes CO with the surface reaction constant of 0.070 m/s at 800K. The pressure is $1.15 \times 10^5\ Pa$ and the mean molecular weight of exhaust gases is 29. Calculate the CO reduction at a location where CO mole fraction is 0.187%.

Assume fully developed profile for mass transfer. Then from the Tables we find that limiting value of Sherwood number is 2.98.

$$D_{CO-air} = 1.1 \times 10^{-4}\ m^2/sec$$

$$\text{Equivalent diameter} = \frac{(4)(L^2)}{4L} = L = 1\ mm$$

$$\frac{k_x\, d_h}{D} = 2.98$$

$$k_x = 2.98\,\frac{x\,1.1\times10^{-4}}{1\times10^{-3}} = 0.0298\,\frac{m}{sec}$$

The surface reaction rate constant is $0.070\,\frac{m}{sec}$. The overall rate constant is obtained by adding the two resistances in series

$$k = \left[\frac{1}{k_s} + \frac{1}{k_s}\right]^{-1} = 0.021\,\frac{m}{sec}$$

Mass transport contributes 70% resistance (verify).

The rate of CO oxidation is then given as follows:

$$R = k\,C_{bulk}\;y_{CO} = (.021)(1.5)\,5.9\times10^{-4} = 0.315\,\frac{g\;mole}{m^2\;\sec}$$

$$C_{bulk} = \frac{P}{RT} = \frac{1\times10^5}{8.314\times800} = 15\,\frac{mole}{m^3}$$

PACKED BEDS

For flow of gases in packed beds, an appropriate correlation for heat transfer coefficient is

$$Nu = \left(0.5\,Re^{1/2} + 0.2\,Re^{2/3}\right)Pr^{1/3}$$

Note: u_g = superficial velocity = $\frac{\dot{m}}{\rho A_c}$

$$V_g = \frac{u_g}{\varepsilon_B} = \frac{\dot{m}}{\rho\varepsilon_B A_c} = \text{interstial velocity}$$

Re is defined as $\frac{VL\rho}{\mu}$

$$Nu = \frac{hL}{R}$$

The pressure drop in packed bed is usually calculated from the Ergun equation

$$\frac{dP}{dx} = \frac{150\,\mu V_g}{L^2} + \frac{1.75\,\rho V_g{}^2}{L}$$

where L is a characteristic length parameter defined as:

$$L = dp\left(\frac{\varepsilon_B}{1-\varepsilon_B}\right)$$

The first term in the Ergun equation accounts for the viscous drag while the second term accounts for the form (inertia) drag.

For non-spherical particles, use $d_p = \frac{6V_p}{A_p}$, i.e. an equivalent diameter.

Matlab Solutions to Diffusion-reaction problems

See pdf file on web.

-=----------

References:

1. M.P. Allen, D.J. Tildeslay, Computer Simulation of Liquids (Clarendon, Oxford, 1987)
2. J. Cortes, E. Valencia, J. Phys. Chem. B. 2004, 108, 2979-2986
3. O. Korluke, W. von Niessen, Surface Science, 401 (1998) 185-198